Original citation:
Beattie, Shane D., Loveridge, Melanie, Lain, Michael J., Ferraria, Stefania, Polzin, Bryant, Bhagat, Rohit and Dashwood, R. J.. (2016) Understanding capacity fade in silicon based electrodes for lithium ion batteries using three electrode cells and upper cut-off voltage studies. Journal of Power Sources, 302. pp. 426-430.

Permanent WRAP URL:
http://wrap.warwick.ac.uk/85960

Copyright and reuse:
The Warwick Research Archive Portal (WRAP) makes this work of researchers of the University of Warwick available open access under the following conditions.

A note on versions:
The version presented in WRAP is the published version, or, version of record, and may be cited as it appears here.

For more information, please contact the WRAP Team at: wrap@warwick.ac.uk

Understanding capacity fade in silicon based electrodes for lithium-ion batteries using three electrode cells and upper cut-off voltage studies

CrossMark

Shane D. Beattie [a, *], M.J. Loveridge [a], Michael J. Lain [a], Stefania Ferrari [a], Bryant J. Polzin [b], Rohit Bhagat [a], Richard Dashwood [a]

[a] WMG, University of Warwick, Coventry, CV4 7AL, United Kingdom
[b] CAMP (Cell Analysis, Modelling and Prototyping) Facility and Support group at Argonne National Laboratory, 9700 South Cass Avenue, Argonne, IL 60439 USA

HIGHLIGHTS

- End of charge voltage drifts more positive as a function of cycle number.
- Voltage at the cathode reaches >4.4 V vs. Li, resulting in capacity fade.
- End of charge voltage dramatically affects cycling efficiency.
- Loss of capacity causes rise in end of charge voltage.

GRAPHICAL ABSTRACT
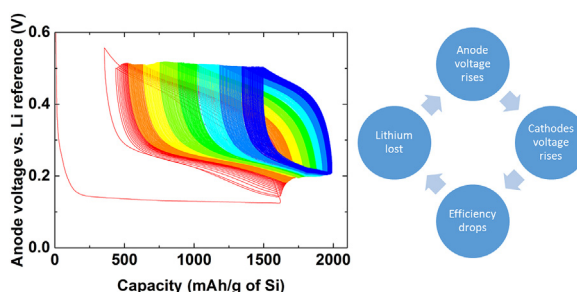
ARTICLE INFO

ABSTRACT

Commercial Li-ion batteries are typically cycled between 3.0 and 4.2 V. These voltages limits are chosen based on the characteristics of the cathode (e.g. lithium cobalt oxide) and anode (e.g. graphite). When alternative anode/cathode chemistries are studied the same cut-off voltages are often, mistakenly, used. Silicon (Si) based anodes are widely studied as a high capacity alternative to graphite for Lithium-ion batteries. When silicon-based anodes are paired with high capacity cathodes (e.g. Lithium Nickel Cobalt Aluminium Oxide; NCA) the cell typically suffers from rapid capacity fade. The purpose of this communication is to understand how the choice of upper cut-off voltage affects cell performance in Si/NCA cells. A careful study of three-electrode cell data will show that capacity fade in Si/NCA cells is due to an ever-evolving silicon voltage profile that pushes the upper voltage at the cathode to >4.4 V (vs. Li/Li$^+$). This behaviour initially improves cycle efficiency, due to liberation of new lithium, but ultimately reduces cycling efficiency, resulting in rapid capacity fade.

1. Introduction

Silicon (Si) is often studied as an alternative to graphite for negative electrodes in Lithium-ion (Li-ion) battery technology due to its high theoretical specific and volumetric capacity (3579 mAh/g

* Corresponding author. Warwick University, International Digital Laboratory, Coventry, CV4 7AL, United Kingdom.
E-mail address: s.d.beattie@warwick.ac.uk (S.D. Beattie).

and 2190 mAh/cm^3 respectively) [1]. Although encouraging theoretically, practical silicon electrodes exhibit relatively low cycle efficiency; capacity retention drops off quickly as a function of cycle number. There are numerous factors which conspire to reduce cycle life in silicon electrodes. Some of the most important factors to consider are:

1) Large expansion during lithiation (up to 280%) [1].
2) Electrode delamination from the current collector due to large volume changes
3) Instability of the Solid Electrode Interphase (SEI) due to large expansion
4) Instability of the electrolyte with lithiated silicon

Factors two and three above are strongly dependent on factor one. A popular strategy to cope with the large expansion associated with full lithiation of silicon is to cycle electrodes to less than full capacity [2–8]. This is often achieved using capacity constrained cycling methodologies in half cells vs. a lithium (Li) metal electrode. For example, some authors restrict the Si capacity to ~1200 mAh/g (instead of 3579 mAh/g) [2–8] and then cycle to ~ 1 V to delithiate the silicon (in half cells). Inevitably, the delithiation capacity is less than the lithiation capacity, due to irreversible capacity loss. As an example, consider cycle x where the silicon electrode is lithiated to 1200 mAh/g. During the subsequent delithiation cycle, suppose that 1195 mAh/g of capacity is recovered (e.g. 99.6% efficiency). In this case 5 mAh/g of capacity is lost, due to irreversible processes, causing 5 mAh/g worth of silicon to become unavailable (e.g. due to loss of electrical contact). On cycle x + 1, the silicon electrode is again lithiated to 1200 mAh/g. This is possible, because both electrodes have an excess of reactant. There is an excess of lithium from the lithium electrode, and there is an excess of silicon (because the silicon is being cycled to 1200 mAh/g, rather than the full capacity of 3579 mAh/g). For simplicity, assume 5 mAh/g of capacity is lost on every cycle. In this case the silicon electrode will be unable to achieve 1200 mAh/g of capacity after 475 cycles. When plotting cycle number vs. capacity, cycles 1–475 will look perfectly flat, then capacity will quickly fall (with a slope of 5 mAh/g/cycle). This type of behaviour is observed in all capacity constrained cycling results [2–8]. Refer to [1], for a more detailed explanation of this process.

Although capacity constrained cycling produces aesthetically pleasing graphs when capacity is plotted as a function of cycle number, it is easy to underestimate the inefficiencies occurring in the cell. This cycling technique masks the true behaviour of the electrode, and is not useful as a practical screening technique.

Despite the considerations above silicon electrodes are commonly cycled to less than their full capacity [2–8]. One method to achieve a type of constrained capacity cycling is to pair a high capacity silicon electrode with a lower (areal) capacity cathode. The cell is charged to a set voltage (e.g. 4.2 V), liberating a known amount of lithium from the cathode. Typically, sufficient cathode material is used to achieve reversible silicon electrode capacities of ~1200 mAh/g (as above).

Silicon electrodes are often fabricated from polycrystalline or semi-crystalline powders. During the first lithiation cycle crystalline Si is converted to amorphous Si. Room-temperature electrochemical lithiation of silicon does not follow the thermodynamic phase diagram [9], [10]. When cycling strategies use less than the full capacity of the silicon it is important to understand what happens to the silicon electrode as a whole, especially as a function of cycle number and state of charge (SOC). Ideally, the unlithiated silicon is a passive spectator, and is not involved during subsequent cycles. However, the spectator theory is not correct. The silicon electrode undergoes gradual but continuous changes during cycling. The data below will also show that changes at the anode

results in detrimental changes at the cathode. A combination of these factors readily explains the rapid capacity fade observed in silicon-based electrodes.

2. Experimental

Silicon electrodes were prepared in multiple steps, outlined below:

2.1. Stock PAA solution

A solution of Polyacrylic Acid (PAA; Sigma Aldrich, MWT = 450 k, purity $\geq$ 99.5%) was prepared by mixing 24 g of PAA with 176 g of deionised water (equates to 12 w/w% PAA) in a 500 mL Nalgene$^®$ beaker. The PAA slurry was mixed using a Primix Homodisper (Model 2.5) at 500 rpm for 120 min, followed by stirring at 250 rpm for a further 120 min with a Primix medium shear impeller blade until the solution was clear.

2.2. Partially neutralised PAA solution

12.4 g of sodium carbonate (Na_2CO_3; Fisher Chemical, purity > 99.5%) was added to the stock PAA solution (described above). This represents a molar ratio of 1.42:1 PAA: Na_2CO_3 and 70% Na neutralization of the PAA. The mixture was stirred by hand, with a spatula, until all of the Na_2CO_3 was dissolved. The partially neutralized Na-PAA solution was left overnight until the Na-PAA solution turned clear. Note that the reaction of the stock PAA solution with Na_2CO_3 was aggressive and excessing foaming occurred.

2.3. Si slurry

10 g of Si (Elkem Silgrain e-Si, d50 3.1 μm, purity 99.7%) was mixed with 1.43 g of carbon black (Alfa Aesar, Acetylene Black purity 99.9+ %, S.A. 75 m^2/g), 0.85 g of graphite (Timrex SFG6, purity 99.93%), and 20 g of deionized water in a 250 mL Pyrex$^®$ vessel. The Si slurry was then placed in a sonic bath (Fisherbrand FB 15060, 150 W, 37 kHz) for 1 h to break down agglomerates. After sonication the slurry was further mixed using medium sheer stirring in a Primix Homodisper Model 2.5 for 30 min at 1000 rpm.

15.45 g of partially neutralized Na-PAA solution (described above) was added to the entirety of the Si slurry described above. The composite slurry was impeller stirred (Primix Homodisper Model 2.5) for 30 min. Thirty millilitres of the resulting solution was transferred to a Filmix mixing vessel and subjected to the following mix cycle: two dispersions for 30 s each at 10 m/s then 30 s at 25 m/s. The rest of the slurry receives the same mixing procedure (the solution was broken up into two smaller batches to accommodate the 60 mL volume of the Primix Homodisper Model 2.5).

The above formulation results in electrodes with a dry mass % composition of 70: 14: 10: 6 (Silicon: Na-PAA: carbon black: graphite).

After degassing, anode coatings were cast onto 10 μm thick Cu foil (Oak Mitsui, electrodeposited) using an RK printing applicator applying a partial vacuum on the Cu foil and a doctor blade set at a blade gap of 100 μm. Coated electrodes were dried on a hot plate at 80 °C followed by vacuum drying (7 mBar) for 12 h at 70 °C.

The mass loading on dried Si electrodes was ~20.7 g/m^2 total and ~14.5 g/m^2 active (i.e.: ~5.2 mAh/cm^2 at full Si capacity).

2.4. Cathode

Lithium Nickel Cobalt Aluminium Oxide, LiNi$_{0.8}$Co$_{0.15}$Al$_{0.05}$O$_2$ (NCA), cathodes were paired with silicon electrodes due to their

high gravimetric capacity (~180 mAh/g). NCA electrodes were prepared by Argonne National Labs (ANL). The ANL cathode was made with a PVdF binder (8%/w) and 84% active material with 4% SFG 6 (Timcal/Imerys) and 4% Super P Li (Timcal/Imerys). Electrode thickness was 87 μm with 25.9% porosity. The areal gravimetric capacity was 18.53 mg/cm^2 with a specific reversible capacity of 150 mAh/g at a rate of 1C (full capacity in 1 h) (i.e.: 2.33 mAh/cm^2).

2.5. Electrolyte

The electrolyte consisted of 1.2 M LiPF$_6$ in 1:3 v/v ethylene carbonate (EC): ethyl methyl carbonate (EMC) with 15% fluoro-ethylene carbonate (FEC) and 3% vinylene carbonate (VC) (Soulbrain). The proper choice of electrolyte formulation is very important to ensure high coulombic efficiency and long cycle life. Standard electrolytes used with graphitic anodes are not optimized for silicon based electrodes. Additives like VC and FEC have been found to be particularly important to increase capacity retention in Si based electrodes [11,12]; hence their use here.

2.6. Three-electrode cells

Three-electrode cells were fabricated using stainless steel Swagelok hardware and perfluoroalkoxy (PFA) ferrules. A ½" T-union was used as the cell body with a plastic insert (fabricated by MicroPlas Mouldings Ltd, The Old Tractor Shed, Heath Farm, Heath Road East, Petersfield, Hampshire GU31 4HT). Two ½" stainless steel plungers were used as supports for the working and counter electrodes. One of the plungers uses a spring and spacer to apply continual pressure on the electrodes (similar to [13]-Fig. 1). The anode and cathode plungers were orientated facing each other (as in Ref. [13]). 12 mm diameter discs of anode/cathode were cut using a precision punch (fabricated by MicroPlas Mouldings Ltd). 12 mm glass fiber separators (Whatman GF/A CAT No. 1820-110) were cut using the same punch. The anode/cathodes were attached to the ends of the plungers and lined up in approximately the center of the T-union body. 50 μL of electrolyte was dispensed with a precision micro-pipette into the body of the T-union. A piece of Li was attached to the end of the top plunger and inserted until flush with the GF/A separator between the anode/cathode. All Swagelok nuts and PFA ferrules were installed the tightened with a torque wrench.

2.7. Two electrode cells

Two electrode cells were fabricated in 2032 coin cell hardware from Hohsen. The cathode cans were coated with a thin layer of aluminium. Celgard 2325 was used as the separator (17 mm diameter). 30 μL of the electrolyte above was dispensed onto the separator. 16 mm diameter anode/cathodes were cut using a precision punch (fabricated by MicroPlas Mouldings Ltd). Three 0.5 mm thick spacers and a wave spring were used to make up the extra volume in the cell. The cell was crimped and tabs spot welded to the cells to minimize contact resistance.

All cell components were dried in a vacuum oven (Binder Vacuum Drying Ovens with integrated vacuum pump system) at 50 °C overnight before assembly.

Connections to the three electrode cell were made using a Biologic VMP3. The stainless steel plungers in have holes drilled for 4 mm banana plugs on the exterior. The white (reference) wire was attached to the Li/Li$^+$ reference electrodes while the red/blue wires were connected to the cathode/anode respectively.

Two electrode cells were cycled with a VMP3 (Biologic) in two-electrode mode (reference electrode shorted to the working electrode) and 2 mm banana plugs soldered to the welded tabs.

2.8. Cycling procedure

The three-electrode cell was charged (lithiation of Si) at a constant C/20 rate (C representing the full capacity of the cathode to 4.2 V) then held at 4.2 V until the current dropped to C/80 (constant current − constant voltage cycling; CCCV). The cell was then cycled at C/2 between 3 and 4.2 V, holding at 4.2 V until the current dropped to C/8 (CCCV). Cell voltage and anode/cathode voltages relative to the Li/Li$^+$ reference were recorded as a function of time/capacity using the Biologic VMP3 EC-Lab software.

Two electrode cells used the same cycling procedure above with different upper cut-off values (see below).

3. Results and discussion

Fig. 1a shows cell voltage as a function of cumulative capacity for over 300 cycles. Capacity is quoted relative to the active mass of the silicon electrode. The colour (online) shift of the voltage curve from red to blue indicates increasing cycle number. This colour scheme is used for all graphs in Fig. 1. There are numerous important features in Fig. 1a. First, the cell has a continual shift to higher and higher capacities. This can be interpreted in a number of ways:

1) Redox reactions are occurring in the cell that appear as capacity drift
2) Excess lithium could be liberated from the cathode during cycling, depending on the voltage profile (more on this later)
3) Irreversible losses due to electrolyte decomposition or lithium isolation
4) A systematic error in the cycling hardware. The Biologic VMP3 unit has a quoted accuracy of <0.1% full scale range (FSR)

The continual shift to higher capacities (walking to the right) is no doubt due to a combination of the considerations mentioned above. It is difficult to isolate the contributions due to irreversible losses, although there are strategies to accomplish this [14]. Hardware errors can be minimized with the proper equipment [15—18]. Regardless of capacity creep, much can be learned from the evolution of the voltage profile [1]. Fig. 1a shows that the capacity window continues to shrink with cycle number, associated with cycle capacity loss.

Most cells are cycled in a two electrode format. However, data from two electrode cells can be difficult to interpret. It's not always clear which electrode is contributing to changes in cell performance. Furthermore, the change in performance is often due to contributions from both electrodes, making it difficult to isolate specific contributions from each. The use of three electrode cells allows the anode/cathode voltage profile to be studied independent of one another (Fig. 1b−c). Three electrode cell data will be discussed next.

The first cycle (red) in Fig. 1b (Si anode voltage vs. Li/Li$^+$ reference vs. capacity) shows a flat voltage profile during the first charge, associated with lithiation of crystalline Si [1]. After the first cycle the sloped voltage profile represents the de/lithiation of amorphous silicon, as expected. An important consideration is the large first cycle capacity (~1600 mAh/g of Si) vs. subsequent cycles (~1200 mAh/g of Si). A significant amount of crystalline Si has been converted to amorphous Si (up to 1600 mAh/g worth), but only a portion of the amorphous Si is being cycled (1200 mA h/g).

Fig. 1c shows the cathode (NCA) voltage vs. the Li/Li$^+$ reference as a function of cumulative capacity. As in Fig. 1b the end of charge voltage increases as a function of cycle number. This rise in end of charge voltage at the cathode is vital to understand capacity fade. Also, the cell suffers from polarization due to the cathode surface being affected by the rise of potential (vs. Li/Li+). On the first cycle
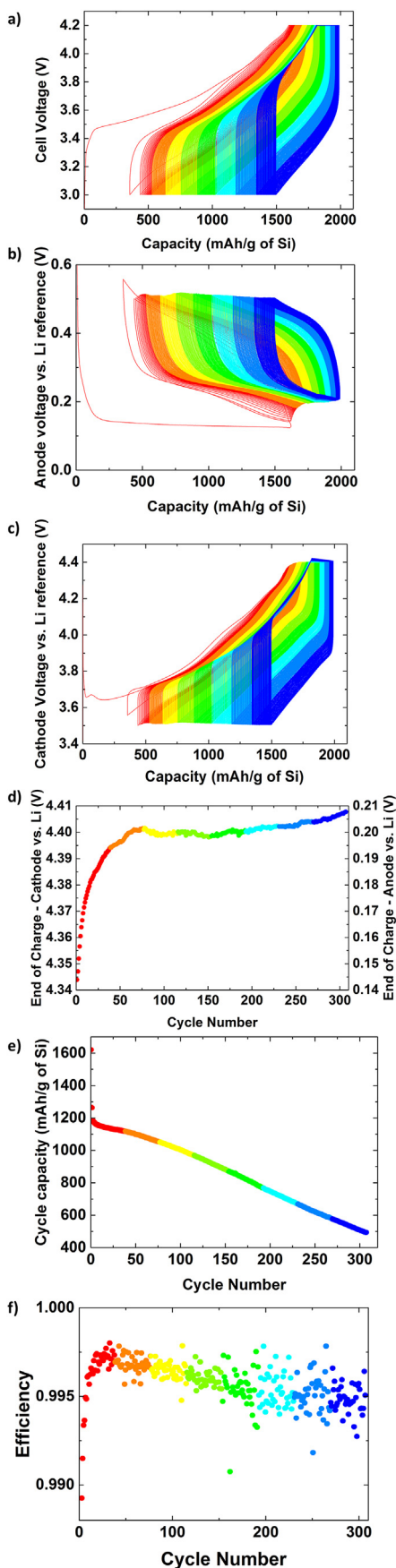
the cathode experiences voltages as high as 4.34 V vs Li/Li$^+$. As the cycle number increases towards 300 the end of charge voltage increases to as high as 4.41 V vs. Li/Li$^+$, which is well beyond the recommended voltage cycling regime of NCA. Electrolyte stability will also be compromised at these voltages [19].

Fig. 1d shows end of charge voltage at the anode/cathode as a function of cycle number. The end of charge voltage rises rapidly for the first ~50 cycles, then stabilizes, but continues to rise as a function of cycle number. More on this behaviour later.

Fig. 1e shows capacity fade as a function of cycle number. The initial capacity is near 1600 mAh/g, but drops to ~1200 mAh/g on the first few cycles. This represents a significant first cycle loss of 25% (which is too large for commercial applications). First cycle loss is due to formation of the Solid Electrode Interphase (SEI) on the surface of the electrode particles, changes in the charge voltage at each electrode (Fig. 1d) and the change to a higher C-rate (from C/20 to C/2).

Fig. 1f shows efficiency vs. cycle number. The first few cycles have an efficiency well below 0.99. The initial cycle efficiencies are not shown in Fig. 1f to allow a smaller efficiency range to be displayed on the y-axis. This smaller y-axis range emphasizes the drop in efficiency as a function of cycle number at later cycles. It is useful to plot efficiency on a scale where small changes in cycle efficiency are clearly evident. A scale of 0–1 is not useful. It is important to understand efficiency values near 1, not 0.

In order to achieve hundreds of cycles with minimal capacity loss a cell must cycle at well over 99.9% efficiency. The cell in Fig. 1f has a maximum cycle efficiency of ~99.8%, which continues to decrease as a function of cycle number. There is more going on in the efficiency data than is obvious at first glance. Consider the rise in cathode voltage as a function of cycle number in Fig. 1d. As the end of charge voltage at the cathode rises, more Li will be liberated from the cathode. This will increase cell efficiency (Fig. 1f), as 'new' Li is being added to the system. Although Li inventory is constantly being consumed due to irreversible processes (e.g. efficiency <1.00 in Fig. 1f), some of the lost Li is being replenished due to the increased charge voltage at the cathode. This artificially increases cell efficiency. In fact, Fig. 1f shows that efficiency rises during the first ~50 cycles. This rise in efficiency tracks well with the rise in end of charge voltage in Fig. 1d, corresponding to new Li being liberated on each cycle. However, when cathode materials are cycled to high voltages (>4.2 V), cycle efficiency will drop; the higher the voltage, the lower the efficiency, the faster the capacity fade.

In summary, as the voltage profile evolves over hundreds of cycles (Fig. 1b–c) the end of charge voltage increases as a function of cycle number (Fig. 1d). When the cathode is charged to higher voltages 'new' lithium is liberated from the cathode, artificially increasing cycle efficiency (Fig. 1f). Higher voltages at the cathode ultimately result in lower cycling efficiency, resulting in rapid capacity fade (Fig. 1e).

To understand the cause of the rise in end of charge voltage consider Fig. 2. During the first lithiation cycle crystalline silicon is converted to amorphous silicon. This is associated with a relatively flat voltage profile. On the delithiation cycle, the voltage profile is sloped. The next lithiation (charge) profile is also sloped. The lower voltage reached at the anode depends on the amount of active lithium inventory in the system. If there is sufficient active lithium inventory to achieve 1200 mAh/g of Si, the end of lithiation (charge) voltage will be low (e.g. 0.14 V; Fig. 2). If the

Fig. 1. a) Cell voltage vs. Si capacity, b) Si vs. Li reference vs. Si capacity, c) NCA vs. Li reference vs. Si capacity, d) End of charge voltage at the anode/cathode vs. Li reference vs. cycle number, e) Capacity vs. cycle number, f) Efficiency vs. cycle number.
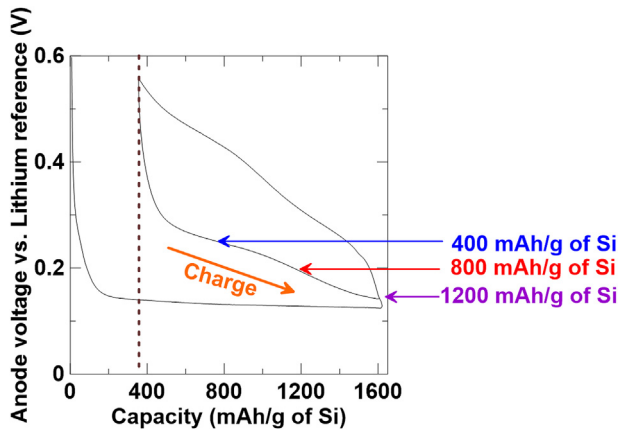
Fig. 2. Effect of lithiation capacity on end of charge voltage at the anode.

active lithium inventory is closer to 800 mA h/g of Si (Fig. 2), the end of lithiation (charge) voltage will be ~0.2 V. If the active lithium inventory is closer to 400 mAh/g of Si (Fig. 2), the end of lithiation (charge) voltage will be ~0.25 V. This rise in end of charge voltage at the anode is significant, because it has a direct effect on the end of charge voltage experienced at the cathode. The charge voltage is dictated by the cycling profile. In this case 4.2 V. If the anode voltage is at 0.25 V at the end of charge, the cathode voltage will be at 4.45 V (4.2 V = 4.45 V−0.25 V). This is one of the dangers associated with using conventional cycling parameters with unconventional cell chemistries. Higher voltages at the anode result in higher voltages at the cathode. Higher voltages at the cathode (>4.2 V) result in lower cycling efficiency. This is why the voltage profile of anode materials should be as low (vs. Li/Li$^+$) as possible.

To explore the relationship between cell upper cut-off voltage and cycle efficiency consider Fig. 3. Four identical two-electrode coin cells (Si vs. NCA as above) were fabricated and cycled using the same procedure as above, but with different upper cut-off voltages: 4.0, 4.1, 4.2, 4.3 V Fig. 3 shows that lower efficiencies result from higher charge voltage values, although the difference between 4.0 and 4.1 V is minimal. The data shows that NCA (like most cathodes) is very sensitive to the upper cut-off voltage. This is especially true when using an anode with a sloping voltage profile (like Si), and rapid capacity fade. Note that graphite does not have a
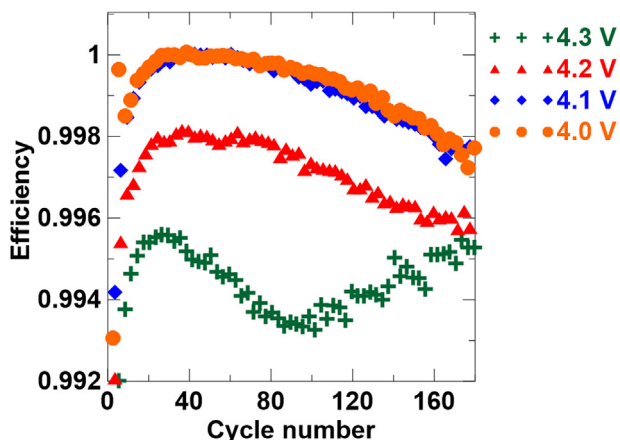
sloping voltage profile, so loss of Li inventory does not result in the same rise in cathode end of charge voltage as in Si-based electrode systems.

4. Conclusion

When studying new electrode chemistries it is important to understand how industry standard cycling profiles (e.g. 3.0−4.2 V) affect cell performance. This is especially true when using electrodes that have high (e.g. > 0.2 V vs. Li/Li$^+$) lithiation profiles. Assuming a 4.2 charge voltage, if the anode voltage at the end of charge is > 0.2 V, vs. Li/Li$^+$ the cathode voltage will be at > 4.4 V vs. Li/Li$^+$. Most cathodes do not cycle with high efficiency above 4.4 V vs. Li/Li$^+$, and electrolyte degradation is accelerated at higher voltages.

Silicon electrodes have a sloping voltage profile. During cycling capacity is lost on every cycle. As capacity is lost there is less active lithium available on the next charge/discharge cycle. If less Li is reacting with the silicon electrode less of the voltage profile is accessed, increasing the end of charge voltage. This rise in charge voltage at the cathode will initially result in new lithium being liberated from the cathode. The higher charge voltage replenishes some of the lithium lost in previous cycles. However, there is a price to pay for the newly liberated lithium. Higher voltages at the cathode results in lower cycling efficiencies, causing capacity fade, which further increases the end of charge voltage. These phenomenon are self-propagating:

1) Less than 100% efficiency results in loss of capacity
2) Loss of capacity results in higher end of charge voltages
3) High end of charge voltages results in lower cycle efficiency
4) Lower efficiency results in loss of capacity
5) Back to 2

This publication and many like it show that commercialization of bulk crystalline silicon electrodes is highly unlikely. The authors encourage researchers to focus their attention on more viable systems like nano-structured silicon alloys.

Fig. 3. Efficiency vs. Cycle number for different end of charge voltages.

References

[1] M. Obrovac, L. Krause, J. Electrochem. Soc. 154 (2007) A103−A108.
[2] D. Mazouzi, Z. Karkar, C. Reale Hernandez, P. Jimenez Manero, D. Guyomard, L. Roué, B. Lestriez, J. Power Sources 280 (2015) 533−549.
[3] G. Talla, R.K. Guduru, B.Q. Li, P.S. Mohanty, Solid State Ionics 269 (2015) 8−13.
[4] M. Ling, Y. Xu, H. Zhao, X. Gu, J. Qiu, S. Li, M. Wu, X. Song, C. Yan, G. Liu, S. Zhang, Nano Energy 12 (2015) 178−185.
[5] B.P.N. Nguyen, S. Chazelle, M. Cerbelaud, W. Porcher, B. Lestriez, J. Power Sources 262 (2014) 112−122.
[6] E. Radvanyi, W. Porcher, E. De Vito, A. Montani, S. Franger, S. Jouanneau Si Larbi, Phys. Chem. Chem. Phys. 16 (2014) 17142−17153.
[7] D. Mazouzi, B. Lestriez, L. Roué, D. Guyomard, Electrochem. Solid-State Lett. 12 (2009) A215−A218.
[8] Y. Oumellal, N. Delpuech, D. Mazouzi, N. Dupre, J. Gaubicher, P. Moreau, P. Soudan, B. Lestriez, D. Guyomard, J. Mater. Chem. 21 (2011) 6201−6208.
[9] J. Li, J. Dahn, J. Electrochem. Soc. 154 (2007) A156−A161.
[10] T. Hatchard, J. Dahn, J. Electrochem. Soc. 151 (2004) A838−A842.
[11] C. Xu, F. Lindgren, B. Philippe, M. Gorgoi, F. Björefors, K. Edström, T. Gustafsson, Chem. Mater. 27 (2015) 2591−2599.
[12] V. Etacheri, O. Haik, Y. Goffer, G.A. Roberts, I.C. Stefan, R. Fasching, D. Aurbach, Langmuir 28 (2012) 965−976.
[13] M. Ender, A. Weber, I.-T. Ellen, J. Electrochem. Soc. 159 (2011) A128−A136.
[14] L. Krause, L. Jensen, J. Dahn, J. Electrochem. Soc. 159 (2012) A937−A943.
[15] J. Burns, G. Jain, A. Smith, K. Eberman, E. Scott, J. Gardner, J. Dahn, J. Electrochem. Soc. 158 (2011) A255−A261.
[16] A. Smith, J. Burns, D. Xiong, J. Dahn, J. Electrochem. Soc. 158 (2011) A1136−A1142.
[17] A. Smith, J.C. Burns, X. Zhao, D. Xiong, J. Dahn, J. Electrochem. Soc. 158 (2011) A447−A452.
[18] A.J. Smith, J.C. Burns, J.R. Dahn, Electrochem. Solid-State Lett. 13 (2010) A177−A179.
[19] J.B. Goodenough, Y. Kim, Chem. Mater. 22 (2009) 587−603.